Published online 1 August 2007 *Nucleic Acids Research, 2007, Vol. 35, No. 15* ***5213–5222***
doi:10.1093/nar/gkm531

Modeling and structure function analysis of the putative anchor site of yeast telomerase

Neal F. Lue* and Zhaohui Li

Department of Microbiology & Immunology, W. R. Hearst Microbiology Research Center, Weill Medical College of Cornell University, 1300 York Avenue, New York, NY 10021, USA

Received June 4, 2007; Accepted June 25, 2007

ABSTRACT

Telomerase is a ribonucleoprotein reverse transcriptase responsible for extending one strand of the telomere terminal repeats. Unique among reverse transcriptases, telomerase is thought to possess a DNA-binding domain (known as anchor site) that allows the enzyme to add telomere repeats processively. Previous crosslinking and mutagenesis studies have mapped the anchor site to an N-terminal region of TERT, and the structure of this region of *Tetrahymena* TERT was recently determined at atomic resolutions. Here we use a combination of homology modeling, electrostatic calculation and site-specific mutagenesis analysis to identify a positively charged, functionally important surface patch on yeast TERT. This patch is lined by both conserved and non-conserved residues, which when mutated, caused loss of telomerase processivity *in vitro* and telomere shortening *in vivo*. In addition, we demonstrate that a point mutation in this domain of yeast TERT simultaneously enhanced the repeat addition processivity of telomerase and caused telomere elongation. Our data argue that telomerase anchor site has evolved species-specific residues to interact with species-specific telomere repeats. The data also reinforce the importance of telomerase processivity in regulating telomere length.

INTRODUCTION

Telomerase is a ribonucleoprotein (RNP) that is responsible for maintaining the terminal repeats of telomeres in most organisms (1–5). The catalytic core of telomerase consists minimally of two components: an RNA in which the template is embedded (named TER in general and TLC1 in the budding yeast *Saccharomyces cerevisiae*), and a reverse transcriptase (RT)-like protein that mediates catalysis (named TERT in general and Est2p in yeast). In addition, telomerase from different organisms have been shown to possess a number of accessory or regulatory subunits that promote telomerase RNP assembly, recruitment and activity.

Though the template region of telomerase RNA typically contains no more than two copies of the telomere repeat, telomerase is known to add long tracts of telomeric DNA to a given primer following a single binding event (6,7). The enzyme is also capable of extending telomeres *in vivo* by multiple repeats in a single cell cycle (8,9). The ability of telomerase to mediate repetitive copying of the template RNA requires two types of processivity: nucleotide addition processivity (NAP), defined as propensity of the enzyme to add nucleotides successively as the template RNA is moved through the active site; and repeat addition processivity (RAP), defined as propensity of the enzyme to initiate another round of copying when the active site reaches the 5′ boundary of the template (7,10). RAP has been postulated to require an interaction between telomerase and the more 5′ region of DNA primer, one that is distinct from the interaction at the catalytic site (11–13). This 'anchor site' interaction is thought to allow telomerase to remain bound to DNA in between rounds of template copying, when the DNA product presumably unpairs from the RNA template. A substantial body of evidence now implicates an N-terminal domain of TERT (known variously as GQ, RID or TEN) as the anchor site. For example, mutations in this domain of yeast and human TERT selectively impair RAP and alter the ability of telomerase to utilize primers in a length- and sequence-dependent manner (14–16). In addition, this region of yeast and *Tetrahymena* TERT can bind DNA with low affinity when recombinantly expressed and purified (17,18). Finally, the same domain of yeast and *Tetrahymena* TERT can be crosslinked to the 5′ region of the DNA primer in the context of a telomerase-primer complex (15,17). However, the detailed molecular mechanisms by which anchor site promote DNA binding and continuous polymerization is not understood.

Recently, Jacobs *et al*. crystallized and determined the structure of the N-terminal domain of *Tetrahymena*

*To whom correspondence should be addressed. Tel: + 212 746 6506; Fax: + 212 746 8587; Email: nflue@med.cornell.edu

© 2007 The Author(s)
This is an Open Access article distributed under the terms of the Creative Commons Attribution Non-Commercial License (http://creativecommons.org/licenses/by-nc/2.0/uk/) which permits unrestricted non-commercial use, distribution, and reproduction in any medium, provided the original work is properly cited.

TERT (17). The structure revealed a single globular domain with a novel fold consisting of 4 β strands and 7 α helices. Well-conserved residues were found to be scattered on two surfaces. Further biochemical analysis demonstrated the importance of an invariant Gln residue in promoting telomerase activity and DNA binding. Somewhat surprisingly (in light of the 'anchor site' notion), mutating this Gln residue (and several other residues) severely reduced overall activity of *Tetrahymena* telomerase *in vitro*, but did not impair its processivity. Thus, the study not only provides the first detailed structural framework for analyzing a critical telomerase protein domain, but also raises interesting questions concerning the precise mechanism of this domain. In the current report, we build on the observations of Jacobs *et al*. and constructed a model of the homologous domain in yeast TERT. Electrostatic calculation revealed two positively charged surface patches, both of which were found to be functionally important through site-specific mutagenesis analysis. Importantly, mutations of residues lining one of the patches (including the invariant Gln and several non-conserved residues) specifically impaired the RAP of yeast telomerase. Even a mild reduction in RAP is correlated with significant telomere loss. Moreover, we found that a previously identified point mutation in the anchor site domain of yeast TERT simultaneously enhanced RAP of telomerase and provoked telomere elongation (19). Our data reveal specific molecular features of the yeast TERT N-terminal domain that are required for function, and suggest that telomerase anchor site has evolved species-specific residues to interact with species-specific telomere repeats. The results also reinforce the importance of telomerase processivity in regulating telomere length.

EXPERIMENTAL PROCEDURES

Homology Modeling

PSI-BLAST searches were carried out using yeast TERT as the query on the non-redundant protein sequence database at NCBI (20). Five iterations were run using an *E*-value cut off of 0.0001. The sequence hits were compiled into a multiple-sequence alignment using ClustalW v1.83, from which very remote homologs were removed and only the known telomerase reverse transcriptase sequences were selected (21). This purged alignment was then used to create a sequence-based profile to which the *Tetrahymena* template (PDB Id: 2B2A) was aligned, creating a structure-to-profile alignment. Pairwise sequence alignment of the template with the query sequence was retrieved from this structure-to-profile alignment for use in homology modeling.

The homology modeling program NEST was used to construct the yeast model. In particular, the *Tetrahymena* template has two gaps of 10 and 6 residues, respectively, with respect to the query sequence. The equivalent regions of the yeast model were filled with the loop building function in NEST. The final model was evaluated by the programs Verify 3D and Prosall, which score structures according to how well each residue fits into its structural environment based on criteria derived from statistical analysis of high-resolution structures in the PDB (22–24). The yeast model was judged to be of good quality and found to superimpose well to the *Tetrahymena* template with an RMS deviation for the backbone atoms of 0.8 Å (Supplementary Figure 1C). The electrostatic properties of the TERT GQ domains were calculated with a modified version of the program Delphi and visualized in the program GRASP, as previously described (25,26).

Yeast strains, plasmids and plasmid shuffle

Plasmid pRS426-EST2 was made by cloning a PCR fragment containing EST2 and 400 bp of flanking sequences in between the Bam HI site and Sac I site of pRS426. Plasmid pSE-EST2-C874, containing a protein A-tagged *EST2* gene, has been described (27). This fully functional Est2p is designated wild type telomerase throughout the text. All substitution mutations in the GQ domain of *EST2* were generated by using the QuikChange protocol (Stratagene), appropriate primer oligonucleotides and pSE-EST2-C874 as template. All point mutations were confirmed by sequencing. A 'plasmid shuffle' strategy was used to assess the functionality of *EST2* mutants. First, pRS426-EST2 was introduced into an *est2*-Δ strain to restore telomere length. Subsequently, the pSE-EST2 series of plasmids were transformed into the strain. The strains bearing both plasmids were grown briefly in YPD and then streaked on 5-FOA-containing plates to select for clones that have lost pRS426-EST2. The colonies were then re-streaked multiple times and monitored for growth defects and telomere length alterations.

Analysis of telomere length

Chromosomal DNAs were isolated from successive streaks of yeast clones bearing wild type and mutant *EST2* genes using the 'Smash and Grab' protocol, digested with PstI, and electrophoretically separated on a 0.9% agarose gel. Following capillary transfer to nylon membranes, telomere-containing fragments were detected by hybridization with a ^{32}P-labeled poly(dG-dT) probe (27).

Assay for yeast telomerase

Whole cell extracts and IgG-Sepharose purified telomerase were prepared as previously described (15,27). Each primer extension assay was carried out using 15 µl of IgG-Sepharose pretreated with 4 mg of protein extract, and was initiated by the addition of a 15 µl cocktail containing 100 mM Tris–HCl, pH 8.0, 4 mM magnesium chloride, 2 mM DTT, 2 mM spermidine, primer oligodeoxynucleotides and varying combinations of labeled and unlabeled dGTP and dTTP. Primer extension products were processed and analyzed by gel electrophoresis as previously described. The oligodeoxynucleotide primers used for telomerase assays were purchased from Sigma-Genosis and purified by denaturing gel electrophoresis prior to use. The primers have the following sequences: TEL15, TGTGTGGTGTGTGGG; OXYT1, GTTTTGGGGTTTTGGG; TEL15(m4,5), TGTGTGGT GTCAGGG.

For determination of the processivity of substitution mutants, assays were performed using OXYT1 or TEL15(m4,5) as primer. The signal for each product was determined by PhosphorImager (Molecular Dynamics) and normalized to the amount of transcript by dividing against the number of labeled residues. The OXYT1 primer ends in 3 Gs, and can align to only one site along the yeast RNA template, thus supporting the addition of a 7-nucleotide sequence (TGTGGTG) up to the 5′ boundary of the template. For nucleotides beyond the +7 position, we assume a sequence of TGTG... (Calculations were made assuming other compatible sequences, and the conclusions were not altered.)

$$\text{Processivity } P_i = \sum_{j=i+1}^{N} (T_j) / \sum_{j=i}^{N} (T_j),$$

where T_i denotes the amount of transcript calculated for the primer + i position and N is the highest number such that a visible signal can be discerned in the PhosphorImager file for the primer + N product. RAP is defined as P_7, i.e. the processivity at the point of translocation.

Protein and RNA analysis

The levels of protein A-tagged yeast TERT in cell extracts were determined by enrichment on IgG-Sepharose and subsequent western blotting as previously described (18). The levels of TERT-associated TLC1 RNA were determined by semi-quantitative RT-PCR using 2X RT-PCR Master Mix (USB Corp.) and primers designed to amplify an ~300 bp product (TLC509: GCAAAGTTTGCACG AGTT and TLC793R: CTTTTTGTAGTGGGATTTA TTC).

RESULTS

Construction and analysis of a homology model of the putative anchor site from yeast TERT

To engage in a structure-based analysis of the yeast telomerase GQ domain, we first constructed a homology model of this domain using the structure of *Tetrahymena* domain as the template. The alignment of the template and target sequence is a critical step in generating a high-quality model, the accuracy of the modeled structure being greatly dependent on the quality of the alignment (28). Because the level of sequence homology between these domains of yeast and *Tetrahymena* TERT is only 14%, we used a structure-to-profile alignment approach (which incorporates sequence information from many family members) to obtain the optimal sequence alignment (see Materials and Methods Section and Supplementary Figure 1). The pairwise sequence alignment between the yeast TERT GQ domain and the *Tetrahymena* template was then extracted from the structure-to-profile alignment and used in the modeling program (Supplementary Figure 2A). This alignment approach has demonstrated success in providing the basis for generating high-quality homology models for proteins with limited sequence similarity to the template (29,30). For model building, we utilized the NEST program, which employs rigid-body assembly coupled with loop modeling (31). A recent comparative evaluation of commonly used modeling programs indicates that NEST performs better than or similarly to other programs (32). The final yeast model of the GQ domain was evaluated with Verify 3D and ProsaII and judged to be of reasonable quality (data not shown). The model also superimposed well onto the template with an RMS deviation for the backbone atoms of 0.8 Å (Supplementary Figure 2B). Notably, the yeast model can readily account for some of the prior mutagenesis results. For example, both W115 and G123, which were previously demonstrated to be essential for telomerase function, are likely to be important for the structural integrity of this domain because the former packs into the interior and the latter is located within a tight turn, as glycines often are (Figure 1B).

We then used electrostatic calculation to identify potential DNA-binding sites on the surface of the yeast domain (31). This analysis revealed two positively charged patches separated by a ridge on one face of the domain (Figure 1). Comparable patches can be observed on the surface of the *Tetrahymena* domain (data not shown). The top patch in the yeast domain (named patch 1) is lined by several basic residues including K111, K116 and H119. The bottom patch (named patch 2) contains the invariant Gln (Q146, which is equivalent to Q168 in *Tetrahymena* TERT) as well as R151, N153 and H156. Notably, none of these residues with the exception of Q146 are conserved in *Tetrahymena*.

The positively charged patches are required for telomerase function *in vivo*

Based on modeling and electrostatic calculation, we chose nine residues in the GQ domain of yeast TERT for detailed mutagenesis analysis. Seven of these are located on either patch 1 (K111, K116 and H119) or patch 2 (Q146, R151, N153 and H156). G149 and C152 are also included in the analysis for comparative purposes. G149 is universally conserved and likely to be functionally important. C152 is located next to patch 2 but points away from it, and may therefore be unimportant. A 'plasmid shuffle' strategy was used to generate a set of isogenic yeast strains containing plasmid-borne wild type or mutant *EST2* genes (see Experimental Procedures Section). To facilitate detection and telomerase isolation, the *EST2* genes were all fused to a protein A tag. The strains were propagated by repeatedly restreaking for single colonies on plates, and then assessed for growth and telomere defects.

As shown in Figure 2, of the 10 mutants, only Q146A and G149A (Ala substitution of invariant residues) exhibited severe growth defects by the third re-streak (~80–100 generations after loss of wild type EST2). The Q146E mutant failed to show significant growth defects, suggesting that this substitution is less disruptive. Not surprisingly, all three mutants also manifested severe telomere loss (Figure 2B). Interestingly, despite their lack of growth defects, 4 of the other 7 mutants (K111A,

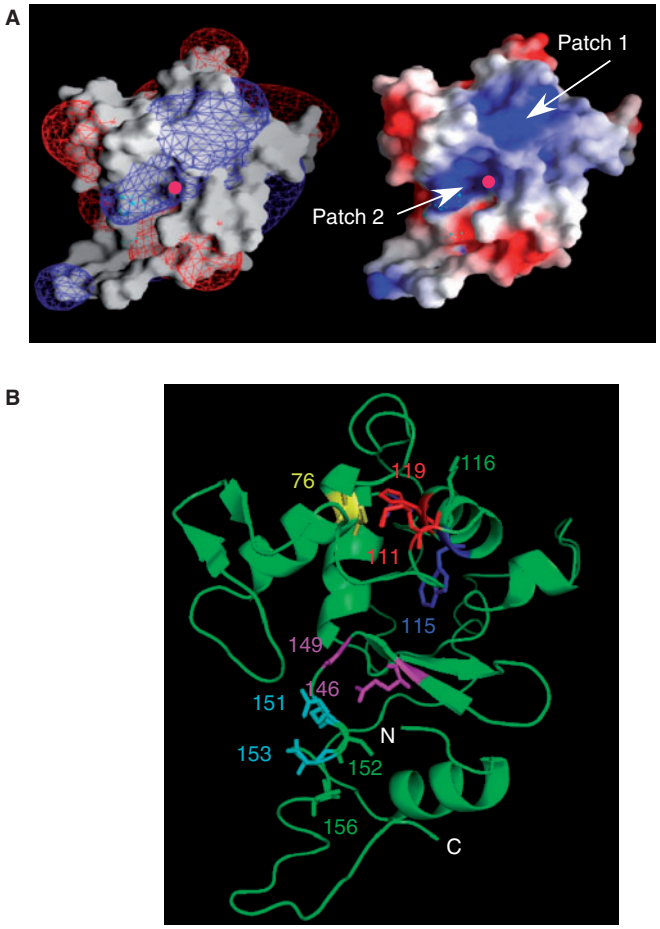

Figure 1. Structure of the putative anchor site of yeast TERT. (**A**) The electrostatic surface potential of the yeast TERT GQ domain is calculated and displayed. Red dots designate the location of the invariant Q146 residue. Two patches with positive electrostatic surface potential are indicated by arrows. (**B**) The residues subjected to mutagenesis are displayed in different colors based on the phenotypes of the mutant: green, no phenotype; red, reduced RNP level; cyan, reduced RAP and magenta, reduced RNP level and RAP. Two other residues noted in this report, W115 and E76, are highlighted in blue and yellow, respectively.

H119A, R151A and N153A) also manifested moderate to severe telomere attrition, indicating that these residues are also functionally important. The remaining three mutants (K116A, C152A and H156A) appear to be functionally intact in their ability to maintain wild type telomere lengths.

Effects of patch mutations on telomerase protein level, RNA association and enzyme activity

To investigate the basis for the observed telomere maintenance defects, we first measured the levels of Est2 protein in the mutant strains. Cell extracts were prepared from the strains and the protein A-tagged Est2p isolated on IgG-Sepharose. The tagged Est2p were then detected using antibodies directed against protein A. As shown in Figure 3A (top panel), different mutations in the GQ domain had different impacts on Est2p protein levels in cell extracts, with H119A and G149A causing the most severe reduction and K111A, Q146A and Q146E causing moderate protein loss. We next assessed the levels of Est2p-associated TLC1 RNA using RT-PCR, and found a correlation between the levels of Est2p and TLC1 RNA in IgG-Sepharose precipitates (Figure 3A, bottom panel). For example, both the H119A and G149A samples showed very low levels of TLC1 RNA, whereas the K111A, Q146A and Q146E samples contained slightly higher levels (but still significantly reduced in comparison with the wild type sample). These findings suggest that mutations in the GQ domain can have a destabilizing effect on either the TERT protein or the telomerase complex.

To further examine the effect of GQ domain mutations, we assayed the levels of telomerase primer extension activity in IgG-Sepharose precipitates using a 15-nt primer with a canonical yeast telomere repeat sequence (Figure 3B). As demonstrated previously by us and others, yeast telomerase is relatively non-processive on this primer and can complete mostly one round of repeat addition, adding up to 7 nt to the starting primer. Again, the amounts of primer extension activity correlated with the levels of Est2p and TLC1 RNA in the IgG-Sepharose precipitates. Thus, none of the mutations seem to impair greatly the catalytic competence of an assembled telomerase complex.

In several previous studies, we demonstrated that yeast telomerase becomes more processive on primers that contain non-yeast telomere sequences (15,27,33). The use of such primers allowed us to identify residues in Est2p that specifically impair RAP. We therefore subjected the newly constructed GQ domain mutants to telomerase assays using one such primer, named OXYT1 (Figure 4A). As expected, wild type telomerase became more processive on this primer and extended it by as many as 18 nt. Interestingly, mutants that exhibited reduced RAP (Q146A, Q146E, R151A, N153A) were all located on patch 2. The alterations for all of the affected mutants were qualitatively similar and can be visualized by comparing the product distribution of the wild type, R151A and N153A enzymes (Figure 4B and C). During the first round of synthesis, the R151A and N153A mutant appear to be slightly more proficient at adding nucleotides successively such that a greater proportion of the extension products reached the +7 length. However, the fraction of products that were further extended by the mutant was significantly reduced, indicative of a clear defect in repeat addition. More specifically, while the WT, R151A and N153A telomerase generated similar amount of +7 product (pre-translocation), the mutant synthesized 50–70% less longer products (post translocation, shaded region). Quantitative analysis revealed statistically significant reductions (~2-fold) in RAP for all of the affected mutants (Figure 4D). In contrast, the K111A, K116A, C152A and H156A mutant were found to have normal RAP. The processivities of the H119A and G149A telomerase were not assessed quantitatively due to low product intensities. To examine the generality of the RAP defect, we performed an additional series of telomerase assays using primer TEL15(m4,5), which also contained non-yeast telomeric sequence. Again, the R151A and

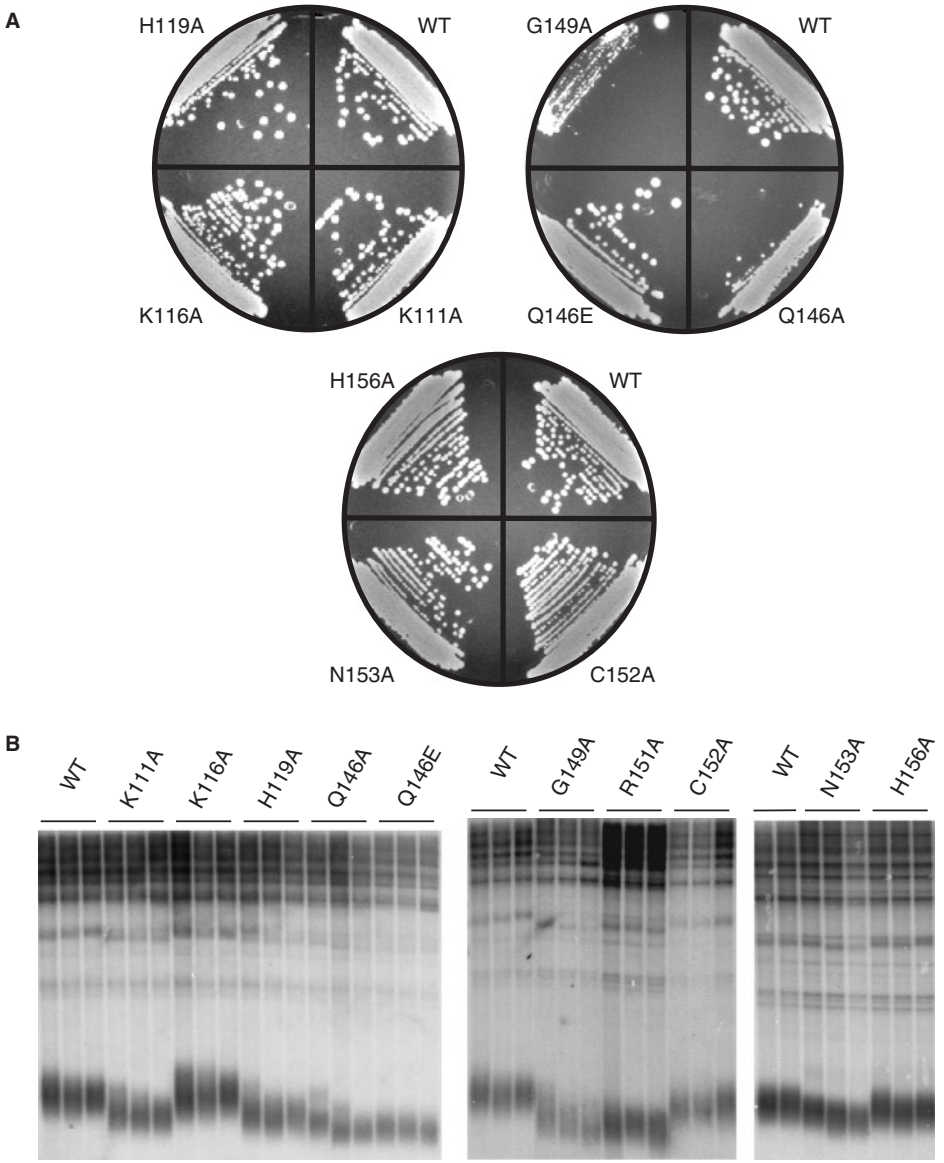

Figure 2. Mutations in the GQ domain impair cell growth and telomere maintenance. (**A**) A 'plasmid shuffle' strategy was used to obtain strains carrying mutated *EST2*. The strains were re-streaked three times and the growth for the third streak shown. (**B**) Chromosomal DNAs were obtained from successive streaks of the yeast strains carrying mutated *EST2*, and checked for telomere length by Southern analysis.

N153A mutation caused significant RAP loss, whereas the C152A and H156A mutation had no effect (Supplementary Figure 3). Together, these findings indicate that residues in the positively charged patch 2 are important for the RAP of telomerase.

In addition to loss of RAP, deletion of the GQ domain was shown previously to result in telomerase with reduced ability to utilize primers [such as OXYT1 and TEL15(m4,5)] that form short hybrids with telomerase RNA (15). To determine if the substitution mutations caused the same defect, we calculated for each mutant the ratio of its activity on the OXYT1 primer to its activity on the TEL15 primer (which can form a long hybrid with telomerase RNA) and normalized the ratio to the wild type enzyme (Figure 4E). Interestingly, we found that all of the patch 2 mutants manifested relative reductions in their activities on the OXYT1 primer. The magnitude of decrease ranged approximately from 2 to 4-fold. A relative reduction in activity was observed as well for the R151A and N153A mutant when the assays were performed using the TEL15(m4,5) primer (Supplementary Figure 3). Thus, the patch 2 mutants evidently exhibited both the primer utilization and processivity defects associated with deletion of the entire GQ domain.

A previously identified mutation in the anchor site region simultaneously provoked telomere elongation and caused an increase in the RAP of telomerase

Ji and colleagues recently described a mutation (E76K) in the anchor site domain of EST2 that caused telomere

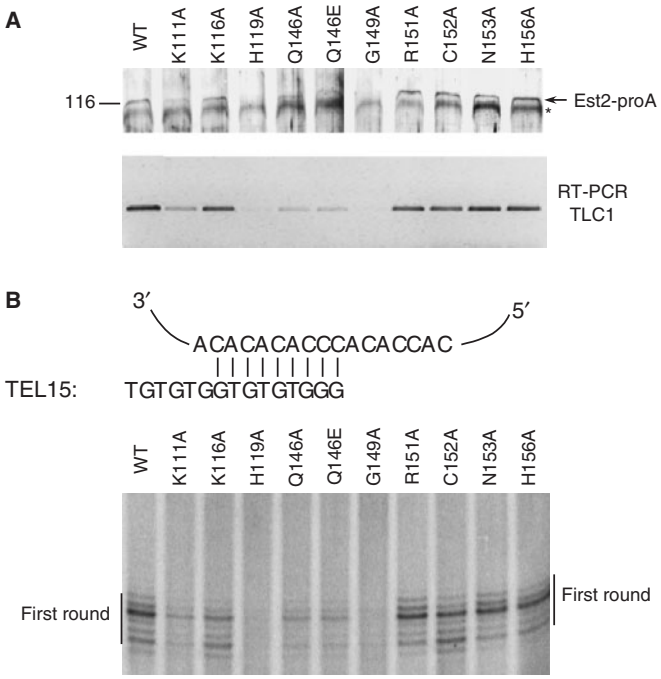

Figure 3. Mutations in the GQ domain lead to reductions in the level of TERT protein, TERT-associated RNA, and telomerase activity. (**A**) (Top) Levels of protein A-tagged Est2p in the mutant extracts were determined by enrichment on IgG-Sepharose and subsequent western blotting using antibodies directed against protein A, and compared to that of the wild type extract. The identities of the mutants are indicated at the top. The position of the protein A tagged Est2p is marked by an arrow on the right. A cross-reacting protein band (∗) can be observed in all of the samples. (Bottom) The levels of Est2p-associated TLC1 RNA in the wild type and mutant strains were determined by semi-quantitative RT-PCR. (**B**) Wild type and mutant telomerase were enriched on IgG-Sepharose and subjected to primer extension assay using TEL15 as the primer in the presence of 50 μM dGTP and 0.3 μM dTTP. The telomerase template RNA and primer sequences are illustrated at the top and a representative set of assays shown at the bottom.

elongation. Based on their studies, they suggest that the mutant is not altered with respect to enzyme activity, but rather abnormal in *TEL1*-mediated regulation (19). However, in their analysis, Ji and colleagues used primers that did not support RAP, making it difficult to determine if the mutation affected this aspect of telomerase property. We therefore decided to re-examine the *in vivo* and *in vitro* functions of this mutant using our system. Consistent with earlier findings, we observed substantial telomere elongation in yeast strains contain the *EST2* E76K allele (Figure 5A). More interestingly, we found that the E76K telomerase exhibited an ~20% increase in RAP relative to WT telomerase (Figure 5B–D). The difference is relatively modest and somewhat difficult to visualize on the PhosphorImager scan (Figure 5B). However, quantitative comparison of the gel lanes showed a significant increase in the relative abundance of the second round products for the E76K enzyme (Figure 5C, compare the blue and red trace in the shaded region). Moreover, the difference is reproducible and statistically significant in different reaction conditions (Figure 5D). For example, the probability of initiating a second round of repeat addition on the OXYT1 primer was 0.55 for WT telomerase and 0.64 for the E76K enzyme when dGTP and dTTP were included at 50 and 0.3 μM, respectively. This difference in RAP was also observed in reactions using 0.3 μM dGTP and 50 μM dTTP (Figure 5D). Notably, this kind of increase was not observed in any other mutants characterized in this study, including the ones that did not induce any telomere length alteration (e.g. H119A, C152A and H156A). We examined a second *est2* mutant reported to induce telomere elongation (N95D). However, in our system, this mutant caused a very mild telomere lengthening phenotype, and we did not observe a statistically significant increase in RAP (Supplementary Figure 4 and data not shown). We conclude that the E76K mutation has a previously undetected effect on the intrinsic enzymatic properties of yeast telomerase, in a manner that is consistent with its ability to induce telomere elongation.

DISCUSSION

Molecular features of yeast telomerase GQ domain required for RAP

The present analyses of the GQ domain of yeast TERT have revealed functionally important residues. Here, we divide the residues into three classes based on phenotypes of the mutants and discuss their mechanisms (see Figure 1B for a visual summary of the results). The first class, including K111 and H119 and located in patch 1, appears to have a 'stabilizing' effect on the telomerase complex; substitution at these positions reduced the levels of RNP and telomerase activity. However, the enzymatic property of telomerase showed no detectable change. The second class, including R151 and N153 and located in patch 2, appears not to be required for telomerase stability, but rather the primer interaction function of GQ domain. Substitution at these positions resulted in loss of activity on primers that form short hybrids with telomerase RNA and loss of RAP. These defects are qualitatively similar to defects exhibited by deletion of the entire GQ domain (15), suggesting that the key function of the GQ domain requires patch 2. While the level of telomerase RNP were reduced slightly in both the R151A and N153A mutant (Figure 3A), it is unlikely that this reduction can account for the telomere shortening phenotype of the mutants; the C152A and H156A mutants suffered slight RNP reduction, yet exhibited no telomere phenotypes. The third class, comprising only of Q146, is apparently required for complex stability as well as primer interaction, because substitution at this position results in the combined phenotype of the first two groups of residues. Thus, despite its surface location, Q146 must mediate important structural as well as enzymatic functions, consistent with its absolute conservation through evolution. Like the R151A and N153A mutant, the senescent and telomere shortening phenotype of the Q146A mutant cannot be attributed to the reduction in RNP level alone because the K111A suffered a comparable degree of RNP loss, yet exhibited only mild telomere shortening. Because all of the functionally important

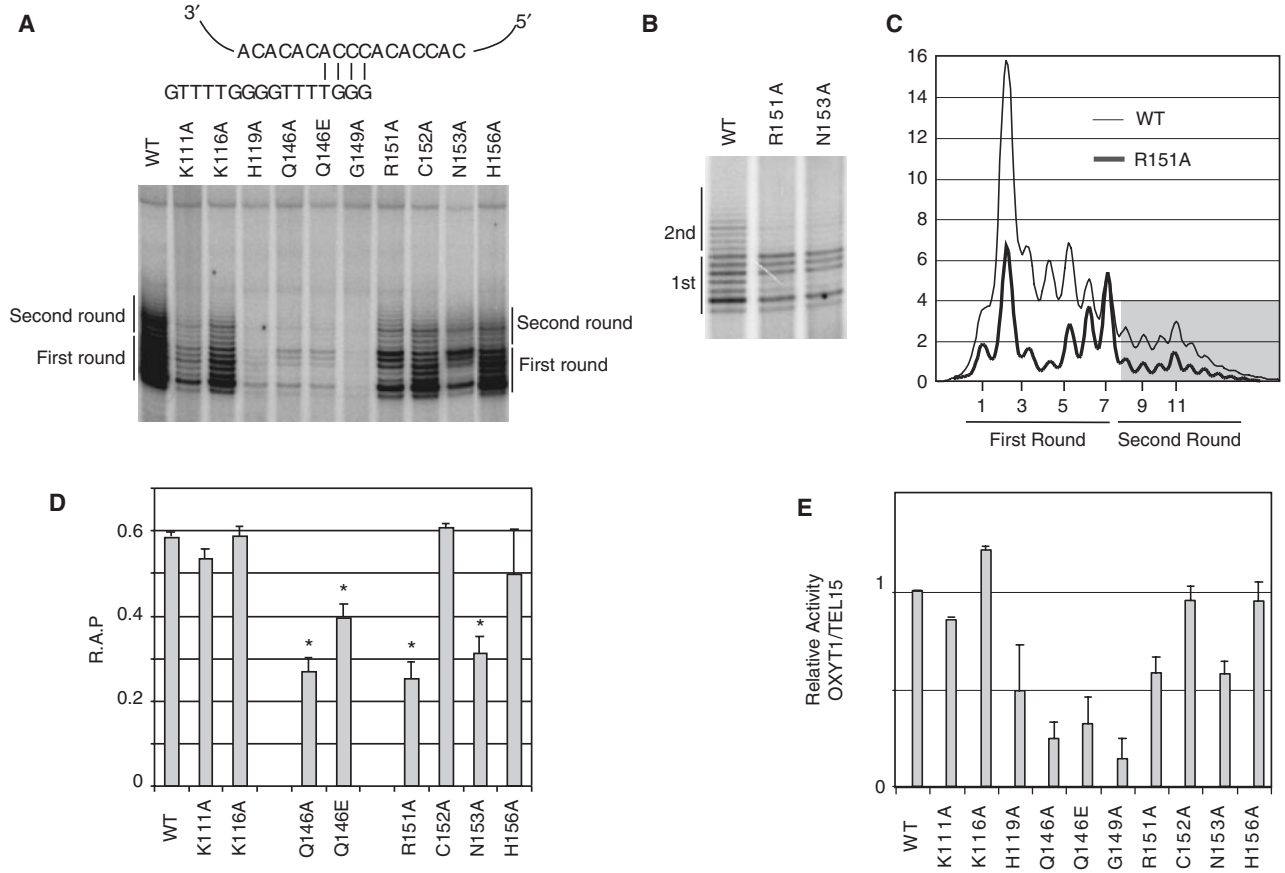

Figure 4. Mutations in the patch 2 results in telomerase processivity and primer utilization defects. (**A**) Wild type and mutant telomerase were enriched on IgG-Sepharose and subjected to primer extension assay using OXYT1 as the primer in the presence of 50 μM dGTP and 0.3 μM dTTP. The telomerase template RNA and primer sequences are illustrated at the top and a representative set of assays shown at the bottom. (**B**) Wild type and mutant telomerase were subjected to primer extension assays as described in part A. To allow for better visual identification of the processivity defect, only 1/2 of the reaction products for the wild type enzyme were applied to the gel. (**C**) The distribution of primer extension products for the wild type and R151A telomerase as shown in part B of this figure were plotted. Note that in this set of assays, comparable amounts of +7 products were generated by both enzymes, but the amount of longer products (in shaded region) was reduced by ~60% for R151A, signifying a loss in RAP. (**D**) The RAP of wild type and mutant telomerase on OXYT1 were determined in triplicate assays and the results plotted. Mutants that exhibited statistically significant reductions in their RAP are marked by asterisks. (**E**) The ratio of the activity of each mutant enzyme on the OXYT1 primer to its activity on the TEL15 primer was determined, normalized to the ratio for the wild type enzyme, and plotted.

residues with the exception of Q146 are not well conserved, our data suggest that telomerase has evolved species-specific residues to mediate important GQ domain functions. This notion is consistent with the high degree of telomere sequence divergence in different organisms. Interestingly, the mutation that confers increased RAP (E76K) does not map near patch 2. Instead, the residue packs against two alpha helices (α5 and α6 in the designation scheme by Jacob *et al.*) that are positioned away from the basic patch (Figure 1B). Thus either other regions of the domain also regulate DNA binding, or the effect of this mutation may be indirect.

Is the conserved GQ domain of telomerase universally required for RAP?

A particularly interesting question raised by previous and current analyses of telomerase in different organisms is whether the contribution of GQ domain to RAP is universally conserved. Such a contribution has been unequivocally demonstrated for the yeast and human domain (15,16,34). However, several analyses of *Tetrahymena* TERT mutants have failed to disclose such a contribution (17,35,36). Indeed, the same mutation in yeast and *Tetrahymena* can apparently have different effects on telomerase enzymology. For example, Ala substitution of the invariant Gln caused a significant reduction in RAP in yeast, but not in *Tetrahymena* (17). The reason for this disparity is not understood, but several potential explanations may be considered. One possibility is that the DNA-binding function of *Tetrahymena* TERT has evolved to serve another aspect of telomerase enzymology, e.g. primer binding during initiation. Alternatively, the presence of other DNA-binding domains or proteins in *Tetrahymena* telomerase may obscure the contribution of the GQ domain to RAP. Finally, it should be noted that all of the *Tetrahymena* studies have been performed using *in vitro* reconstituted telomerase, which differs significantly with respect to

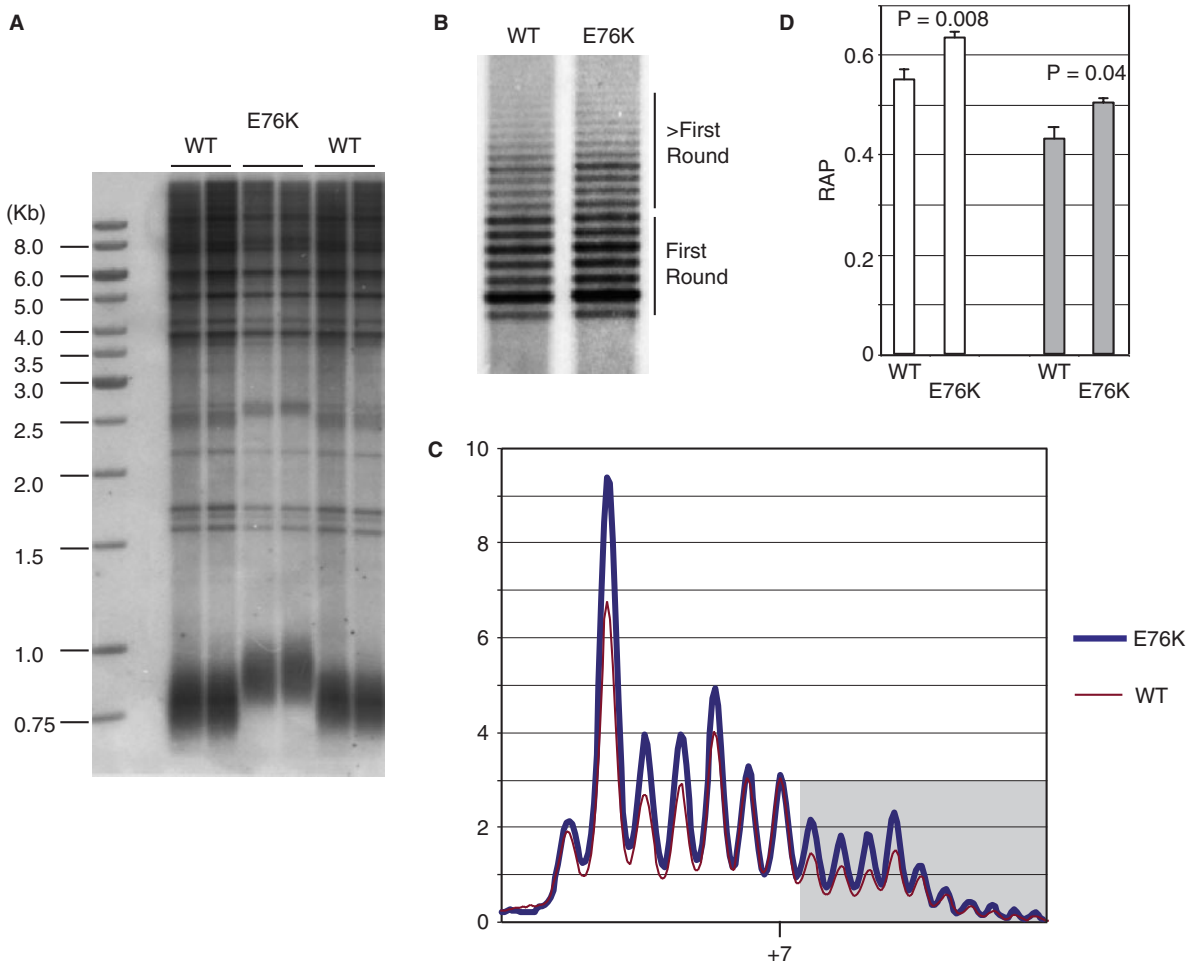

Figure 5. The E76K mutation simultaneously induced telomere elongation and an increase in telomerase processivity. (**A**) Isogenic yeast strains carrying wild type and the E76K allele of EST2 were obtained by plasmid shuffle, streaked twice and their telomere lengths assayed by Southern analysis. (**B**) Wild type and E76K telomerase were enriched on IgG-Sepharose and subjected to primer extension using OXYT1 as the primer in the presence of 50 μM dGTP and 0.3 μM dTTP. The first round and longer than first round products are marked by two vertical bars to the right. Note that there was a moderate increase in the relative level of longer products in the E76K sample, which was reproducibly observed (see part **C** and **D**). (**C**) The distribution of extension products for wild type and E76K telomerase as observed in the assays shown in B are plotted. Note that there is a moderate increase in the levels of longer than +7 products in the E76K sample (in the shaded area), signifying an increase in RAP for this telomerase. (**D**) The RAP of wild type and E76K telomerase on OXYT1 were determined in duplicate or triplicate assays using different concentrations of nucleotides and the results plotted. The blue bars represent results obtained from assays that included 50 μM dGTP and 0.3 μM dTTP, and the red bars from assays that include 0.3 μM dGTP and 50 μM dTTP. The *P*-values of the differences were calculated using paired *t*-test and shown at the top.

processivity from the endogenous enzyme (37–39). In this regard, we note that a protocol for reconstituting mutant *Tetrahymena* telomerase *in vivo* was recently reported (40). It may be interesting to re-examine the contribution of GQ domain to RAP in this presumably more physiologically relevant system.

Implications for telomere extension *in vivo* and telomerase evolution

In earlier studies, we demonstrated that yeast telomerase mutants with reduced and enhanced NAP supported the maintenance of shorter and longer than wild type telomeres, respectively (41). We have also identified mutations that simultaneously impaired RAP and telomere maintenance (27). In this report, we further show that a mutation in the GQ domain of yeast TERT that resulted in increased RAP also induced telomere elongation. Collectively, these data provide strong argument for the notion that the intrinsic processivity of telomerase is an important determinant of telomere length. Furthermore, they support a recently proposed model of telomere length homeostasis (1,8). This model has two key premises. First, there is a feedback loop that regulates the activity of telomerase as a function of telomere length, such that longer telomeres are more refractory to extension. Second, regulation of telomerase activity occurs at the step of initiation rather than processivity. In this model, telomere lengths are at equilibrium when the average shortening rate (SR, dictated by incomplete end replication) is balanced by the average extension rate,

which can be obtained by multiplying the probability of initiation (Pi) with average processivity (E), such that

$$SR = Pi(L) \times E$$

Note that as stated before, Pi is a function of telomere length (L) and is negatively correlated with L. Thus for example, when processivity is enhanced by a telomerase mutation (e.g. the E76K mutation), equilibrium can only be achieved by reducing Pi. A reduction in Pi, in turn, can be achieved by increasing telomere length. Thus, the model predicts an increase in equilibrium telomere length in the presence of a processivity-enhancing mutation, precisely as observed.

The occurrence of yeast telomerase mutants with increased processivity suggests that there is relatively little evolutionary pressure to optimize this aspect of yeast telomerase enzymology. This may be related to the fact that yeast cells have a very low telomere shortening rate (3–4 bp generation) such that a telomerase with low processivity is sufficient to maintain telomere length homeostasis. It is interesting that in some organisms with greater telomere attrition rate (e.g. humans), telomerase has apparently evolved to become more processive, perhaps to discharge the function of maintaining telomere length homeostasis.

SUPPLEMENTARY DATA

Supplementary Data are available at NAR Online.

ACKNOWLEDGEMENTS

We thank Dr. Diana Murray for help with homology modeling and discussions. This work was supported by an R01 from the National Institute of Health (N. Lue). The Department of Microbiology and Immunology at Weill Cornell Medical College gratefully acknowledges the support of the William Randolph Hearst Foundation. Funding to pay the Open Access publication charges for this article was provided by NIH grant GM62631.

Conflict of interest statement. None declared.

REFERENCES

1. Autexier,C. and Lue,N.F. (2006) The structure and function of telomerase reverse transcriptase. *Annu. Rev. Biochem.*, **75**, 493–517.
2. Cech,T. (2004) Beginning to understand the end of the chromosome. *Cell*, **116**, 273–279.
3. Collins,K. (2006) The biogenesis and regulation of telomerase holoenzymes. *Nat. Rev. Mol. Cell Biol.*, **7**, 484–494.
4. Blackburn,E.H. (2005) Telomeres and telomerase: their mechanisms of action and the effects of altering their functions. *FEBS Lett.*, **579**, 859–862.
5. Theimer,C.A. and Feigon,J. (2006) Structure and function of telomerase RNA. *Curr. Opin. Struct. Biol.*, **16**, 307–318.
6. Greider,C. (1991) Telomerase is processive. *Mol. Cell. Biol.*, **11**, 4572–4580.
7. Lue,N. (2004) Adding to the ends: what makes telomerase processive and how important is it? *Bioessays*, **26**, 955–962.
8. Teixeira,M., Arneric,M., Sperisen,P. and Lingner,J. (2004) Telomere length homeostasis is achieved via a switch between telomerase-extendible and -nonextendible States. *Cell*, **117**, 323–335.
9. Marcand,S., Brevet,V., Mann,C. and Gilson,E. (2000) Cell cycle restriction of telomere elongation. *Curr. Biol.*, **10**, 487–490.
10. Collins,K. (1999) Ciliate telomerase biochemistry. *Annu. Rev. Biochem.*, **68**, 187–218.
11. Lee,M. and Blackburn,E.H. (1993) Sequence-specific DNA primer effects on telomerase polymerization activity. *Mol. Cell. Biol.*, **13**, 6586–6599.
12. Collins,K. and Greider,C.W. (1993) Tetrahymena telomerase catalyzes nucleolytic cleavage and nonprocessive elongation. *Genes Dev.*, **7**, 1364–1376.
13. Harrington,L.A. and Greider,C.W. (1991) Telomerase primer specificity and chromosome healing. *Nature*, **353**, 451–454.
14. Beattie,T.L., Zhou,W., Robinson,M.O. and Harrington,L. (2000) Polymerization defects within human telomerase are distinct from telomerase RNA and TEP1 binding. *Mol. Biol. Cell*, **11**, 3329–3340.
15. Lue,N. (2005) A physical and functional constituent of telomerase anchor site. *J. Biol. Chem.*, **280**, 26586–26591.
16. Moriarty,T.J., Ward,R.J., Taboski,M.A. and Autexier,C. (2005) An anchor site-type defect in human telomerase that disrupts telomere length maintenance and cellular immortalization. *Mol. Biol. Cell*, **16**, 3152–3161.
17. Jacobs,S.A., Podell,E.R. and Cech,T.R. (2006) Crystal structure of the essential N-terminal domain of telomerase reverse transcriptase. *Nat. Struct. Mol. Biol.*, **13**, 218–225.
18. Xia,J., Peng,Y., Mian,I.S. and Lue,N.F. (2000) Identification of functionally important domains in the N-terminal region of telomerase reverse transcriptase. *Mol. Cell. Biol.*, **20**, 5196–5207.
19. Ji,H., Platts,M.H., Dharamsi,L.M. and Friedman,K.L. (2005) Regulation of telomere length by an N-terminal region of the yeast telomerase reverse transcriptase. *Mol. Cell. Biol.*, **25**, 9103–9114.
20. Altschul,S.F., Madden,T.L., Schaffer,A.A., Zhang,J., Zhang,Z., Miller,W. and Lipman,D.J. (1997) Gapped BLAST and PSI-BLAST: a new generation of protein database search programs. *Nucleic Acids Res.*, **25**, 3389–3402.
21. Thompson,J.D., Higgins,D.G. and Gibson,T.J. (1994) CLUSTAL W: improving the sensitivity of progressive multiple sequence alignment through sequence weighting, position-specific gap penalties and weight matrix choice. *Nucleic Acids Res.*, **22**, 4673–4680.
22. Sippl,M.J. (1993) Recognition of errors in three-dimensional structures of proteins. *Proteins*, **17**, 355–362.
23. Luthy,R., Bowie,J.U. and Eisenberg,D. (1992) Assessment of protein models with three-dimensional profiles. *Nature*, **356**, 83–85.
24. Bowie,J.U., Luthy,R. and Eisenberg,D. (1991) A method to identify protein sequences that fold into a known three-dimensional structure. *Science*, **253**, 164–170.
25. Honig,B. and Nicholls,A. (1995) Classical electrostatics in biology and chemistry. *Science*, **268**, 1144–1149.
26. Nicholls,A., Sharp,K.A. and Honig,B. (1991) Protein folding and association: insights from the interfacial and thermodynamic properties of hydrocarbons. *Proteins*, **11**, 281–296.
27. Lue,N., Lin,Y. and Mian,I. (2003) A conserved telomerase motif within the catalytic domain of telomerase reverse transcriptase is specifically required for repeat addition processivity. *Mol. Cell. Biol.*, **23**, 8440–8449.
28. Venclovas,C. (2001) Comparative modeling of CASP4 target proteins: combining results of sequence search with three-dimensional structure assessment. *Proteins*, (Suppl. 5), 47–54.
29. Liu,G., Li,Z., Chiang,Y., Acton,T., Montelione,G.T., Murray,D. and Szyperski,T. (2005) High-quality homology models derived from NMR and X-ray structures of E. coli proteins YgdK and Suf E suggest that all members of the YgdK/Suf E protein family are enhancers of cysteine desulfurases. *Protein Sci.*, **14**, 1597–1608.
30. Herve du Penhoat,C., Atreya,H.S., Shen,Y., Liu,G., Acton,T.B., Xiao,R., Li,Z., Murray,D., Montelione,G.T. *et al.* (2004) The NMR solution structure of the 30S ribosomal protein S27e encoded in gene RS27_ARCFU of Archaeoglobus fulgidis reveals a novel protein fold. *Protein Sci.*, **13**, 1407–1416.
31. Petrey,D., Xiang,Z., Tang,C.L., Xie,L., Gimpelev,M., Mitros,T., Soto,C.S., Goldsmith-Fischman,S., Kernytsky,A. *et al.* (2003) Using multiple structure alignments, fast model building, and energetic

analysis in fold recognition and homology modeling. *Proteins*, **53**(Suppl. 6), 430–435.
32. Wallner,B. and Elofsson,A. (2005) All are not equal: a benchmark of different homology modeling programs. *Protein Sci.*, **14**, 1315–1327.
33. Bosoy,D. and Lue,N. (2004) Yeast telomerase is capable of limited repeat addition processivity. *Nucleic Acids Res.*, **32**, 93–101.
34. Moriarty,T., Marie-Egyptienne,D. and Autexier,C. (2004) Functional organization of repeat addition processivity and DNA synthesis determinants in the human telomerase multimer. *Mol. Cell. Biol.*, **24**, 3720–3733.
35. Lai,C., Miller,M. and Collins,K. (2002) Template boundary definition in Tetrahymena telomerase. *Genes Dev.*, **16**, 415–420.
36. Lai,C.K., Mitchell,J.R. and Collins,K. (2001) RNA binding domain of telomerase reverse transcriptase. *Mol. Cell. Biol.*, **21**, 990–1000.
37. Collins,K. and Gandhi,L. (1998) The reverse transcriptase component of the Tetrahymena telomerase ribonucleoprotein complex. *Proc. Natl Acad. Sci. USA*, **95**, 8485–8490.
38. Hardy,C., Schultz,C. and Collins,K. (2001) Requirements for the dGTP-dependent repeat addition processivity of recombinant Tetrahymena telomerase. *J. Biol. Chem.*, **276**, 4863–4871.
39. Bryan,T.M., Goodrich,K.J. and Cech,T.R. (2000) A mutant of tetrahymena telomerase reverse transcriptase with increased processivity. *J. Biol. Chem.*, **275**, 24199–24207.
40. Cunningham,D.D. and Collins,K. (2005) Biological and biochemical functions of RNA in the tetrahymena telomerase holoenzyme. *Mol. Cel. Biol.*, **25**, 4442–4454.
41. Peng,Y., Mian,I.S. and Lue,N.F. (2001) Analysis of telomerase processivity: mechanistic similarity to HIV-1 reverse transcriptase and role in telomere maintenance. *Mol. Cell*, **7**, 1201–1211.